Attachment of *Chlamydia trachomatis* L2 to host cells requires sulfation

David M. Rosmarin[a,b], Jan E. Carette[c], Andrew J. Olive[d], Michael N. Starnbach[d], Thijn R. Brummelkamp[e], and Hidde L. Ploegh[a,1]

[a]Department of Biology, Whitehead Institute for Biomedical Research, Cambridge, MA 02142; [b]Department of Dermatology, Brigham and Women's Hospital, Boston, MA 02115; [c]Department of Microbiology and Immunology, Stanford University School of Medicine, Stanford, CA 94305; [d]Department of Microbiology and Immunobiology, Harvard Medical School, Boston, MA 02115; and [e]Division of Biochemistry, The Netherlands Cancer Institute, 1066 CX Amsterdam, The Netherlands

Chlamydia trachomatis is a pathogen responsible for a prevalent sexually transmitted disease. It is also the most common cause of infectious blindness in the developing world. We performed a loss-of-function genetic screen in human haploid cells to identify host factors important in *C. trachomatis* L2 infection. We identified and confirmed *B3GAT3*, *B4GALT7*, and *SLC35B2*, which encode glucuronosyltransferase I, galactosyltransferase I, and the 3′-phosphoadenosine 5′-phosphosulfate transporter 1, respectively, as important in facilitating *Chlamydia* infection. Knockout of any of these three genes inhibits *Chlamydia* attachment. In complementation studies, we found that the introduction of functional copies of these three genes into the null clones restored full susceptibility to *Chlamydia* infection. The degree of attachment of *Chlamydia* strongly correlates with the level of sulfation of the host cell, not simply with the amount of heparan sulfate. Thus, other, as-yet unidentified sulfated macromolecules must contribute to infection. These results demonstrate the utility of screens in haploid cells to study interactions of human cells with bacteria. Furthermore, the human null clones generated can be used to investigate the role of heparan sulfate and sulfation in other settings not limited to infectious disease.

Often leading to pelvic inflammatory disease and infertility, *Chlamydia trachomatis* is the most common bacterial sexually transmitted disease (1). It is also the leading cause of infectious blindness worldwide (2). *Chlamydia* is an obligate intracellular pathogen with a biphasic developmental cycle. The infectious agent is the elementary body (EB). On invasion, the EB differentiates into a metabolically active reticulate body. *Chlamydia* resides entirely within a protected membrane-bound inclusion. Because of this biphasic lifestyle, there is currently no straightforward genetic system with which to manipulate the *Chlamydia* genome. Without the ability to easily knock out, mutate, alter, or add to the *Chlamydia* genome, our knowledge of how *Chlamydia* co-opts host functions remains limited.

Although *Chlamydia* can infect most cultured mammalian cells, the host receptors involved in the uptake of the pathogen have not been definitively identified. An initial reversible interaction, followed by irreversible binding of the EB to the host cell, has been hypothesized (3). The possible role of heparan sulfate as a host factor that contributes to adhesion in *Chlamydia* infection is controversial. Heparan sulfate proteoglycans may be important in the initial reversible interaction of the EB with the host cell (4–6); however, *Chlamydia* infection independent of heparan sulfate has been reported (7). Our genetic screen in a human cell line not only addresses this controversy, but also shows the more general utility of this tool in examining the role of sulfation beyond heparan sulfate.

Past genetic screens for host factors that affect *Chlamydia* infection of mammalian cells have met with limited success. Using chemical mutagenesis, Carabeo et al. (8) isolated a CHO cell clone resistant to *Chlamydia*, and Fudyk et al. (9) found 12 CHO clones that are resistant to *Chlamydia*, but had difficulty identifying the mutations that impart resistance. Only one of the

12 clones initially identified was subsequently characterized as carrying a mutation in protein disulfide isomerase (10). Chemical mutagenesis screens suffer from the fact that a great many genes will be altered because of the dose of mutagen required to obtain a pool of mutants that can be screened. This makes it difficult to connect mutant phenotypes with any particular affected gene.

RNA interference screens also have been used to identify host factors important for *Chlamydia* infection, such as PDGFRβ (11) and the MEK-ERK signaling pathway (12). Despite their widespread use, siRNA screens suffer from off-target effects, and do not always succeed in completely eliminating gene expression. This is of particular relevance when the products of the target genes have enzymatic activity, the complete suppression of which may be required to elicit a phenotype.

We performed a loss-of-function genetic screen in human haploid cells to identify mutant cell lines resistant to *Chlamydia* (13–16). This system avoids the potential off-target effects and incomplete knockdowns of an siRNA screen. It has the advantage over a chemical mutagenesis screen in causing only a limited number of disrupted genes per cell, which can be readily identified by deep sequencing and restored to WT by provision of the corresponding cDNA. An obvious drawback is the false-negatives resulting from the exclusion of genes essential to cell survival. Genes that function redundantly would be equally difficult to isolate as null mutants. We identified three host genes, all of which are involved in the sulfation of host proteins that facilitate *Chlamydia* attachment. By isolating null alleles from the screen, our results demonstrate the importance in *Chlamydia* infection of *B3GAT3*, *B4GALT7*, and *SLC35B2*, which encode glucuronosyltransferase I, galactosyltransferase I, and the 3′-phosphoadenosine 5′-phosphosulfate (PAPS) transporter 1 (PAPST1), respectively. The clone deficient in PAPST1 retains ~5% of its heparan sulfate level, yet is more resistant to *Chlamydia* than the two clones that have no detectable heparan sulfate. Thus, there must be a role for sulfated proteins beyond heparan sulfate as critical mediators in *Chlamydia* attachment.

Sulfation is important for many diverse processes. Lacrimal gland development (17), viability and neural development in *C. elegans* (18), FGF-induced signaling (19), and cartilage homeostasis (20) all depend on sulfation. Sulfation of tyrosine residues is important for the interaction of chemokines and their receptors (21–23) and for binding and entry of HIV (24). Beyond studying interactions of bacteria with human host cells, the tools generated here can be used to investigate in tissue culture other processes

MICROBIOLOGY

in which sulfation may be important. Attempts to reduce expression of SLC35B2 with such methods as RNAi have led to only modest reductions in function, hindering study of the role of sulfation (25). Armed with the isolated null clones, we can now study and better understand many other processes that involve sulfation.

Results

Haploid Genetic Screen Yields Three Gene Candidates Important in *Chlamydia* Infection.

To identify host genes important in *Chlamydia* infection, we used a genetic screen based on the human haploid cell line HAP1 (26) (Fig. 1*A*). The HAP1 cell line is a derivative of the near-haploid leukemia cell line KBM7 generated by transduction with the four reprogramming factors: OCT4, Sox-2, c-MYC, and KLF4. Unlike the KBM7 parental cell line, the majority of HAP1 cells contain a single copy of chromosome 8. The cells grow adherently, and are susceptible to infection with and killed by *C. trachomatis* L2. To find genes important for *Chlamydia*
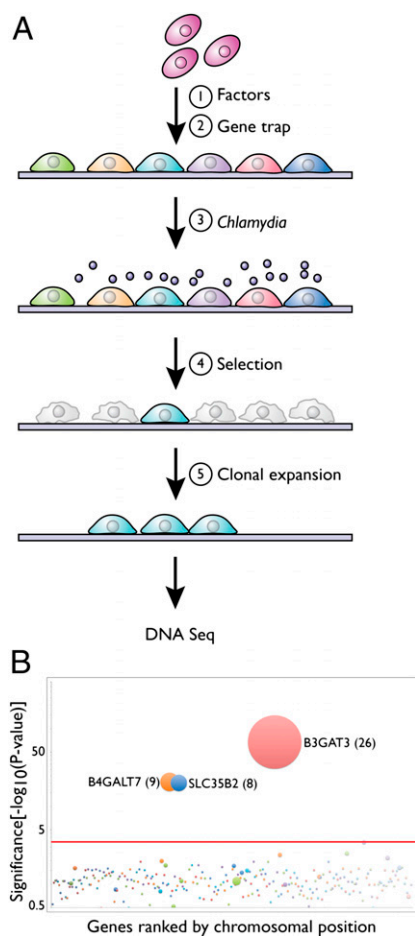

Fig. 1. Loss-of-function haploid genetic screen with *C. trachomatis* L2. (*A*) Outline of the loss-of-function haploid genetic screen with *C. trachomatis* L2; see the text for details. (1) KBM7 cells are reprogrammed to adherent cells by OCT4, Sox-2, c-MYC, and KLF4. (2) HAP1 cells are transduced with the gene trap virus. (3) The mutated cells are inoculated with *C. trachomatis* L2. (4) Virtually all (99.99%) of the mutant cells die from *Chlamydia* infection. (5) Survivors are expanded, the DNA is extracted, and the DNA is sequenced. (*B*) Bubble plot of loss-of-function haploid genetic screen results. The *x* axis shows genes with at least one inactivating mutation ranked in order of chromosomal position. The *y* axis shows the −log of the *P* value of the enrichment of gene-trap insertions in the indicated gene compared with an unselected control dataset. The size of the bubble is correlated with the number of independent insertions. Genes with a *P* value < 0.0001 are labeled, and the number of independent insertions is given in brackets.

cytotoxicity, we mutagenized HAP1 cells with a retroviral gene-trap vector, yielding a heterogeneous cell population with inactivating insertions in nonessential genes containing on average one insertion event per cell (13, 15). Approximately 10^8 mutagenized HAP1 cells were inoculated with *C. trachomatis* L2 at an multiplicity of infection (MOI) of ∼6 and incubated for 5 d, after which 99.99% of the starting pool of mutagenized cells died. After 5 d, antibiotics were added to eliminate any remaining *Chlamydia*. We recovered the surviving cells, which we estimated to total ∼500 clones.

To identify the inactivated genes that permitted survival, we extracted genomic DNA from the resistant clones, performed inverse PCR, and used parallel sequencing with primers flanking the retroviral integration site to map these sites onto the human genome. We compared the frequency of genes enriched for the gene-trap insertions to the frequency of such insertions in unselected but mutagenized control cells (Fig. 1*B*). In the figure, circles represent individual genes; the area of these circles is proportional to the number of independent insertions identified in the resistant mutagenized HAP1 population. Three genes that, when disrupted, provide resistance to *Chlamydia* infection were significantly enriched. *B3GAT3*, *B4GALT7*, and *SLC35B2* were represented with 26, 9, and 8 independent insertions, respectively (respective *P* values of 2.97×10^{-68}, 1.77×10^{-21}, and 7.5×10^{-21}). Although these genes are enriched to a highly significant degree, the screen will not detect some false-negatives or genes important in *Chlamydia* infection, because of the stringency applied and the possibility of redundancy of host proteins. *B3GAT3*, *B4GALT7*, and *SLC35B2* are all involved in the synthesis of glycosaminoglycans such as heparan sulfate. The active site residues of these enzymes are known, allowing the design of vectors that encode catalytically active and inactive variants.

Ectopic Expression of Proteins Encoded by *B3GAT3*, *B4GALT7*, or *SLC35B2* in Their Respective Deficient Hap1 Clones Restores Susceptibility to *Chlamydia*.

We verified the results of the genetic screen as follows. Three independent clones were isolated that carry gene disruptions for the *B3GAT3*, *B4GALT7*, and *SLC35B2* genes. Analysis by gene-specific PCR confirmed that the gene trap indeed interrupted the respective gene in each of the clonal isolates (Fig. S1*A*). We confirmed that no contaminating WT cells remained in our clonal isolates. To further demonstrate that the clones lacked the WT transcripts of the respective genes, we performed RT-PCR and failed to detect the corresponding mRNAs (Fig. 2*A*). We then transduced the null clones with an empty vector; these lines are designated B3GAT3^{GT}, B4GALT7^{GT}, and SLC35B2^{GT}. We restored expression in the null clones with full-length cDNAS encoding the WT products equipped with a C-terminal HA tag; these lines are designated B3GAT3^{GT}+ B3GAT3-HA, B4GALT7^{GT}+B4GALT7-HA, and SLC35B2^{GT}+ SLC35B2-HA. Finally, we transduced the individual mutant clones with enzymatically inactive versions, likewise equipped with a C-terminal HA tag; these lines are designated B3GAT3^{GT}+B3GAT3^{mut}-HA, B4GALT7^{GT}+B4GALT7^{mut}-HA, and SLC35B2^{GT}+SLC35B2^{mut}-HA (Fig. S1*B*).

Retroviral expression of C-terminally HA-tagged B3GAT3, B4GALT7, and SLC35B2 fully restored susceptibility to killing by *Chlamydia*. In contradistinction, HA-tagged enzymatically inactive forms of the encoded gene products did not restore susceptibility to *Chlamydia*, and these clones readily survived beyond 4 d after inoculation with *Chlamydia* (Fig. 2*B*), long after their susceptible counterparts had succumbed. The striking difference in survival between the reconstituted and null clones validates the results of the screen and underscores the importance of *B3GAT3*, *B4GALT7*, and *SLC35B2* in facilitating *Chlamydia* infection.
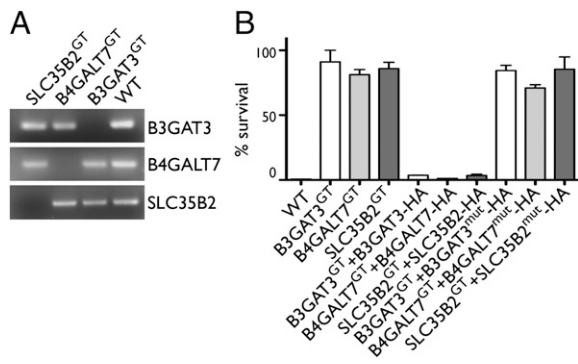
Fig. 2. Cells without *B3GAT3*, *B4GALT7*, or *SLC35B2* are resistant to death by *Chlamydia* infection. (*A*) RT-PCR analysis showing that the isolated null clones SLC35B2^{GT}, B4GALT7^{GT}, and B3GAT3^{GT} do not express any mRNA of their particular gene. (*B*) Bar graph of the survival of null clones inoculated with *C. trachomatis* L2. Retroviral expression of C-terminal HA-tagged B3GAT3, B4GALT7, and SLC35B2 fully restored susceptibility to killing by *Chlamydia*. HA-tagged enzymatically inactive forms of the encoded gene products did not restore susceptibility to *Chlamydia*, and these clones readily survived for 4 d after inoculation with *Chlamydia*.

Time Course of *Chlamydia* Infection in Clones.

We next determined at what stage the genes disrupted in our clones impart resistance to *Chlamydia* infection. Using quantitative real-time PCR, we analyzed a time course of replication of *Chlamydia* within the inclusions. We plotted the increase in DNA in *Chlamydia* versus a host housekeeping gene. At 2 h postinfection, less *Chlamydia* DNA was associated with the null clones, as expected. For the fraction of bacteria that did succeed in establishing a foothold, even in the null clones, *Chlamydia* replicated equally well in the null clones and the reconstituted clones, as inferred from the similar slopes of the plotted growth curves (Fig. 3 *A–C*). The figure shows a downward shift of the curve for the null clones compared with *Chlamydia* growth in the reconstituted clones. Thus, the mechanism of resistance for the null clones most likely involves the attachment/entry phase. If the *Chlamydia* cannot attach to the null clones, then it will be unable to infect the host cells and then kill them. The small fraction of the null clones to which *Chlamydia* attaches are still infected and ultimately die. *Chlamydia* released from the null clones was fully infectious and equivalent in this regard to the *Chlamydia* produced from reconstituted mutant cells, showing that a defect in sulfation pathways in the host cell does not affect growth properties of *Chlamydia* per se. Transmission electron microscopy revealed no obvious ultra-structural differences in the *Chlamydia* inclusions in WT compared with null clones at 36 h postinfection (Fig. 3*D*). Whereas there are fewer inclusions in the null clones, the inclusions that do form are of similar size, and apparently similar numbers of elementary and reticulate bodies contained within them, as inclusions in WT cells (Fig. 3*E*).

Attachment Assay of *Chlamydia* Infection in Isolated Clones.

To confirm that attachment of *Chlamydia* to host cells is affected by the genes discovered in the screen, we compared the number of *Chlamydia* that attach to host cells in the null and reconstituted clones. *Chlamydia* do not attach as well to the null clones compared with their respective reconstituted counterparts (Fig. 4*A*). There is a significant difference in attachment between the reconstituted and null clones for *B3GAT3*, *B4GALT7*, and *SLC35B2*, as measured by quantitative real-time PCR. This also can be visualized via immunofluorescence for the null clones (Fig. 4*B*). We found enhanced resistance to *Chlamydia* attachment in the *SLC35B2* null clone compared with the *B3GAT3* and *B4GALT7* null clones.
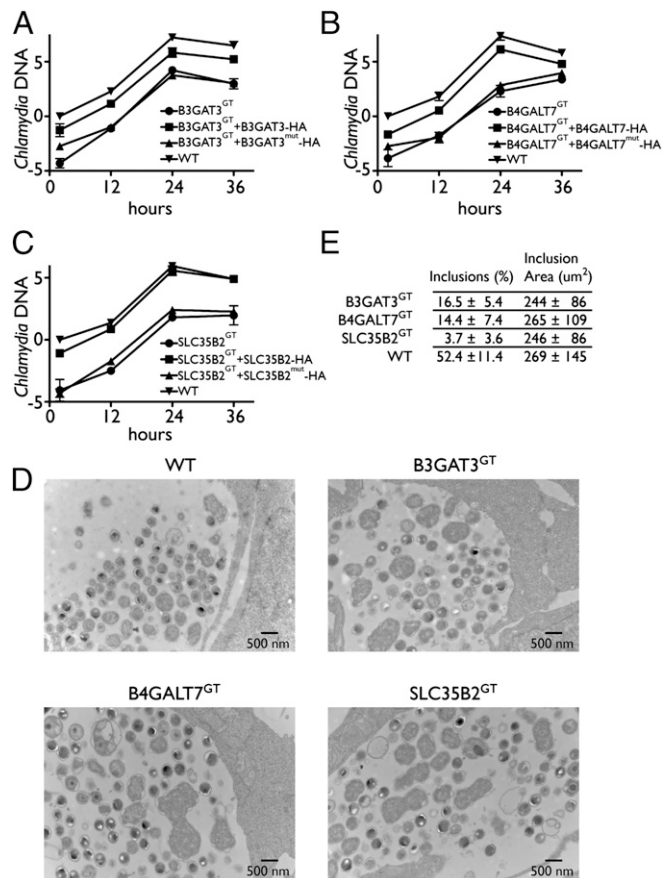

Fig. 3. Although the null clones resist *Chlamydia* infection, the *Chlamydia* that do enter the clones behave similarly to the WT clone. (*A–C*) Time course of *C. trachomatis* L2 replication as measured by *Chlamydia* DNA compared with a housekeeping gene (β-actin). (*D* and *E*) Transmission electron microscopy of WT and null clones (B3GAT3^{GT}, B4GALT7^{GT}, and SLC35B2^{GT}) at 36 h after infection with *C. trachomatis* L2. There were fewer inclusions in the null clones, and the inclusions that were seen were of similar size. The elementary bodies and reticulate bodies had equivalent morphology.

Confirmation That Sulfated Proteins Besides Heparan Sulfate Are Involved in *Chlamydia* Attachment.

We performed an attachment assay to verify significant differences between B3GAT3^{GT} and SLC35B2^{GT}, between B3GAT3^{GT} and B4GALT7^{GT}, and between B4GALT7^{GT} and SLC35B2^{GT} ($P = 0.0418$, $P = 0.0232$, and $P = 0.0139$, respectively, one-sided unpaired *t* test) (Fig. 5*A*). In addition, we harvested *Chlamydia* from the null clones and the reconstituted clones and measured the number of infectious-forming units (IFUs) produced by reinoculating dilutions into McCoy cells (Fig. 5*B*). The differences between B3GAT3^{GT} and SLC35B2^{GT}, between B3GAT3^{GT} and B4GALT7^{GT}, and between B4GALT7^{GT} and SLC35B2^{GT} were significant as well ($P < 0.0001$, $P < 0.0012$, and $P < 0.0002$, respectively, one-sided unpaired *t* test). Because the mechanism of resistance of the null clones is via attachment, we hypothesized that *Chlamydia* co-opts a sulfated product to gain entry into the host cell.

We labeled the individual clones with $^{35}SO_4$ for ~24 h and observed that the SLC35B2^{GT} null clone showed a >90% reduction in incorporation of $^{35}SO_4$ into high molecular weight (MW) materials as resolved by SDS/PAGE. B3GAT3^{GT} and B4GALT7^{GT} were completely deficient in the production of high MW proteins with heparan sulfate, but showed sulfation of other proteins (Fig. 5*C*). The inability of B3GAT3^{GT} and B4GALT7^{GT} to produce any heparan sulfate and the ability of SLC35B2^{GT} clone to still yield heparan sulfate at ~5% of WT levels were
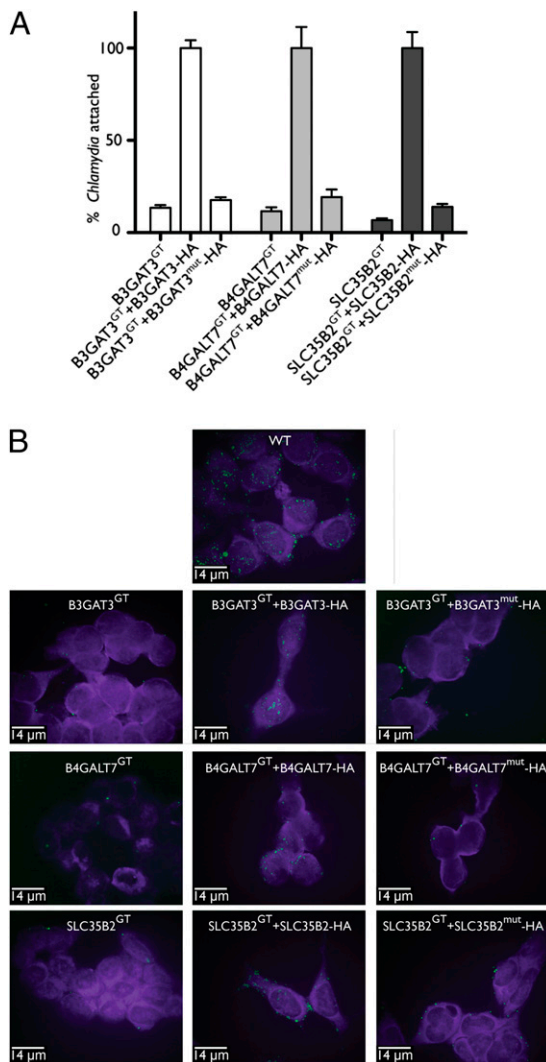
MICROBIOLOGY

Fig. 4. The null clones resist *Chlamydia* attachment. (*A*) Bar graph comparing the attachment of *C. trachomatis* L2 of the null clones and enzymatically inactive reconstituted clones with that of the clones reconstituted with the WT protein. (*B*) Immunofluorescence of the null clones, reconstituted clones with the WT protein, and reconstituted clones with enzymatically inactive mutants after infection with *C. trachomatis* L2 for 1 h at room temperature. The *Chlamydia* elementary bodies are stained with a monoclonal antibody and appear green; the clones are counterstained with Evans blue and appear purple.

confirmed by FACS analysis (Fig. 5*D*). Thus, other sulfated proteins must contribute to *Chlamydia* attachment. On autoradiography of $^{35}SO_4$-labeled cell-associated materials resolved by SDS/PAGE, the reconstituted SLC35B2^{GT}+SLC35B2-HA and WT clones both showed smears at ∼220 KDa (Fig. S2). This material corresponds to heparan sulfate, being heparitinase-sensitive. The SLC35B2^{GT} had only ∼5–10% of the WT levels of heparan sulfate. Other polypeptides are sulfated as well, some of which are sensitive to PNGase F and thus are *N*-glycosylated.

In an effort to extend the foregoing results to a different tissue culture model, we created five stable knockdown cell lines each for the *B3GAT3*, *B4GALT7*, and *SLC35B2* genes, with a GFP knockdown cell line as a control in HeLa cells. The best two knockdowns as determined by RT-PCR are shown in Fig. S3*A*. We measured heparan sulfate levels by FACS analysis using a heparan sulfate-specific antibody (Fig. S3*B*). Some reduction in heparan sulfate levels was seen, but to nowhere near the degree

seen in the null clones. There was little change in *Chlamydia* attachment for the knockdown clones, not nearly to the extent seen for the null clones (Fig. S3*C*). Whether sulfated proteins other than those modified with heparan sulfate contribute to *Chlamydia* attachment cannot be inferred from these knockdown experiments. Thus, obtaining the null clones by insertional inactivation has a significant advantage over the knockdown approach, yielding complete null mutants.

Taken together, our data indicate that there must be sulfated proteins in addition to those carrying heparan sulfate that are deficient in the B3GAT3^{GT}, B4GALT7^{GT}, and SLC35B2^{GT} null clones, any of which may contribute to *Chlamydia* attachment.

Discussion

We have identified and established by several criteria the involvement of three host genes in the facilitation of *Chlamydia* infection. The *SLC35B2* mutation imparts greater resistance to the attachment of *Chlamydia* compared with the *B3GAT3* or *B4GALT7* mutations. Thus, we suggest that the role of sulfated proteins extends beyond the simple provision of heparan sulfate to involvement in *Chlamydia* infection. All of the sulfated proteins present in the reconstituted clones and absent from the null clones are candidates for proteins involved in *Chlamydia* attachment, but their identity remains to be established. Electrostatic interactions also may play a role, given that negatively charged glycosaminoglycans can block adherence of *Chlamydia* to host cells (27).

SLC35B2 encodes PAPST1. PAPS, the universal sulfate donor in biological reactions, is synthesized in the cytoplasm or nucleus by PAPS synthetase and transported into the Golgi by the PAPS transporter for sulfation of proteins (28, 29) by the requisite sulfotransferases. The steady-state labeling of the null *SLC35B2* and reconstituted *SLC35B2* clone with $^{35}SO_4$ demonstrates the importance of a functional PAPST1 in allowing sulfation of cellular proteoglycans, such as heparan sulfate (30). The ∼5% of heparan sulfate remaining in the *SLC35B2* clone may be due to activity of the second PAPS transporter (PAPST2). Chlorate is a competitive inhibitor of PAPS synthetase and blocks sulfation, which partially protects host cells from *Chlamydia* infection (31). However, the high concentrations of chlorate required to block *Chlamydia* infection are toxic to the host cells. Furthermore, F-17 cells deficient in 2-O-sulfation of heparan sulfate show no significant reduction in *C. trachomatis* infectivity compared with WT cells (32). Attempts at knockdown of the PAPST1 gene have achieved no better than a 20% reduction in $^{35}SO_4$ incorporation, even with a 60% reduction in mRNA levels (25). Even low expression levels of PAPST1 leave the cells largely susceptible to *Chlamydia*. A small-molecule inhibitor of PAPST1 may be active against *C. trachomatis* infection. The utility of a loss-of-function screen and the null mutants thus identified is self-evident.

Both *B3GAT3* and *B4GALT7* are important in the synthesis of heparan sulfate and chondroitin sulfate (33–35). CHO cells deficient in enzymes in the heparan sulfate pathway (PgsA-745, PgsD-677, and CHO-761) (4, 36) show decreased infectivity with *Chlamydia* compared with the parental CHO-K1 line. No reconstitution of chemically mutagenized *Chlamydia*-resistant CHO cell lines has been reported, presumably because such lines are heavily mutagenized to begin with, complicating identification of the mutations responsible for resistance. No CHO cell line with a mutation in the PAPST1 transporter has been identified to enable more global study of sulfation.

The CHO-18.4 cell line, derived using a retroviral vector with presumably a single insertion and lacking heparan sulfate, showed no difference compared with parental CHO-22 controls, but the location of this insertion remains unknown (7). Heavily mutagenized CHO-224 cells have a presumed glucuronosyltransferase I mutation and, when complemented, show only a twofold difference in both attachment and infectivity. Our results suggest a more important role of glucuronosyltransferase I in *Chlamydia*
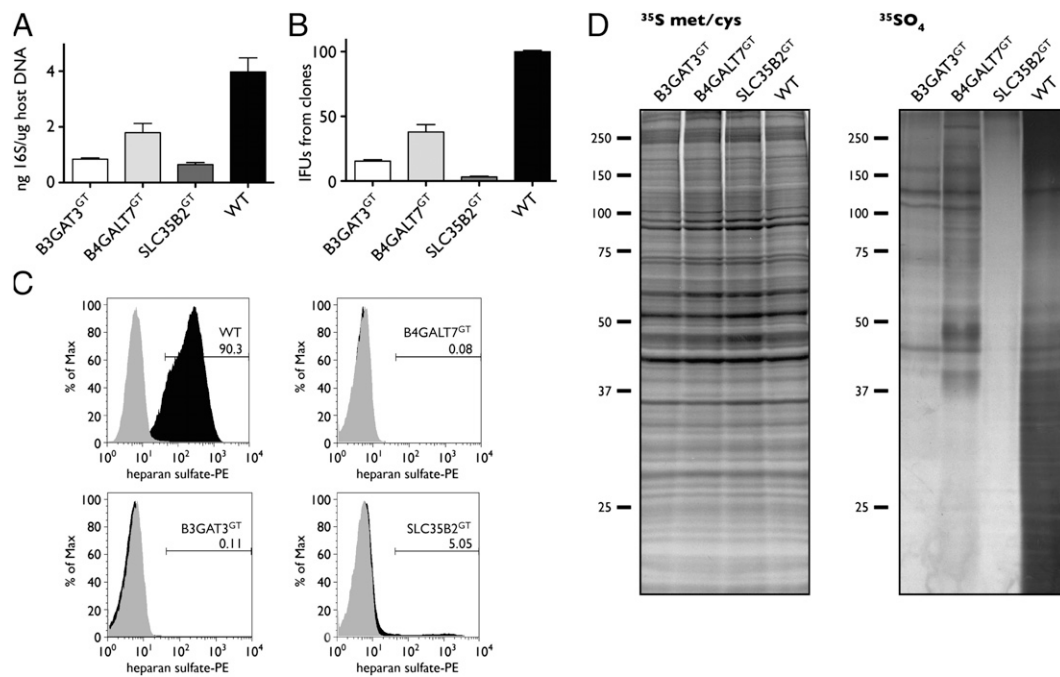
Fig. 5. The importance of sulfation beyond heparan sulfate in *Chlamydia* infection. (*A*) Bar graph comparing the attachment of *C. trachomatis* L2 of the null clones. A one-sided unpaired *t* test shows less attachment of chlamydia to SLC35B2[GT] versus B3GAT3[GT], to B3GAT3[GT] versus B4GALT7[GT], and to SLC35B2[GT] versus B4GALT7[GT] ($P = 0.0418$, 0.0232, and 0.0139, respectively). (*B*) Infectivity of *C. trachomatis* L2 recovered from WT and null clones (B3GAT3[GT], B4GALT7[GT], and SLC35B2[GT]). At 36 h after infection of the clones, *Chlamydia* was harvested and used to inoculate McCoy cells for tittering. *Chlamydia* inclusions were detected by immunofluorescence and enumerated by counting inclusions (IFU). $n = 3$. The differences between B3GAT3[GT] and SLC35B2[GT], between B3GAT3[GT] and B4GALT7[GT], and between B4GALT7[GT] and SLC35B2[GT] are significant by the one-sided unpaired *t* test ($P < 0.0001$, < 0.0012, and < 0.0002, respectively). (*C*) FACS histograms of the null clones and WT clone stained with anti-heparan sulfate antibody before and after heparitinase digestion. The B3GAT3 and B4GALT7 clones are completely deficient in heparan sulfate proteins, whereas the SLC35B2 clone has ~5% of cells positive for heparan sulfate. (*D*) (*Left*) Autoradiogram control showing equivalent incorporation of [35S]met/[35S]cys in the null clones and WT clone. (*Right*) Autoradiogram showing a 90–95% reduction in the incorporation of 35SO$_4$ in the SLC35B2 null clone (SLC35B2[GT]) compared with the WT clone. The SLC35B2 null clone has less sulfated proteins than the B3GAT3 null clone, which has less sulfated proteins than the B4GALT7 null clone.

attachment. Furthermore, FGF2 enhances binding of *Chlamydia* in an heparan sulfate proteoglycan-dependent manner (37). Candidate *Chlamydia* proteins involved in these interactions include the *Chlamydia* OmcB protein, which binds to glycosaminoglycans, such as heparan sulfate (38–40).

Heparan sulfate is believed to be important for many pathogens (41) to allow the infectious cycle to proceed. In the glucuronosyltransferase-deficient CHO cell line, *Toxoplasma* replication is retarded (42). In the clones that we obtained, we observed no deficiency in the ability of *Chlamydia* to replicate in the null clones once access was gained, notwithstanding the deficit in attachment. With the genetic methods as applied to CHO cells and summarized above, it has been difficult to establish functional differences between heparan sulfate and other sulfated proteins as contributors to *Chlamydia* infection. The unique tools that emerge from the present study should facilitate these investigations.

Genes identified on this screen and the isolated clones harboring the individual disruptions may find application in other areas of biology as well. Given that a mutation in *B4GALT7* is linked to a progeroid form of Ehlres–Danlos syndrome (43), it may be worth exploring whether such patients are more resistant to *Chlamydia* infection. For other infectious diseases, including herpes, *Toxoplasma*, *Neisseria*, and HIV, these clones can serve as tools to further examine pathogens' modes of attachment or other aspects of their infectious cycles, which may involve a role for sulfation beyond heparan sulfate. Given the importance of sulfation in controlling the activity of certain G protein-coupled receptors (21–23, 44), the availability of defined mutant cell lines defective in sulfation creates new opportunities that complement

the mutation of putative sulfation sites in the receptors themselves. Should the HAP1 cell line prove amenable to differentiation into more specialized cell types (17), it may even be possible to explore tissue-specific aspects of sulfation.

Materials and Methods

Haploid Genetic Screen. The creation of the haploid HAP1 cell line (26) and the screening procedure have been described previously (13, 15). In brief, the gene-trap retrovirus was created from transfection of low-passage T293 cells. Approximately 100 million HAP1 cells were infected with concentrated gene-trap retrovirus to create a mutagenized library. The mutagenized cells were then inoculated with *C. trachomatis* L2 at an MOI of ~6 and incubated for 5 d. Dead cells were removed by exchanging the spent media for fresh media. After 1 wk, approximately 500 visible *Chlamydia*-resistant colonies were collected. Most of the survivors were unified and grown to 30 million cells after 5 d.

Attachment Assay. The attachment assay was performed by inoculating the clones with an MOI of ~200 at 24 °C for 1 h without centrifugation. The cells were then washed four times. For microscopy, the cells were then fixed with methanol. The *Chlamydia* EBs were stained with an FITC-MOMP, and the HAP1-derived cells were counterstained with Evans blue using the MicroTrak *Chlamydia trachomatis* Kit (Trinity Biotech).

Quantitative PCR. A quantitative PCR assay was performed to quantify attached *Chlamydia* on host cells (45). The nucleic acids were isolated using the QIamp DNA Mini Kit (Qiagen) or High Pure PCR Template Preparation Kit (Roche). Human β-actin DNA and *Chlamydia* 16S DNA were quantified on an Applied Biosystems ABI Prism 7000 sequence detection system using primer pairs and dual-labeled probes. The ratio of the weight of *Chlamydia* to human DNA in the samples was calculated using standard curves from known amounts of *Chlamydia* and human DNA.

Viability Assay. The CellTiter-Glo Luminescent Cell Viability Assay (Promega) was used to quantify the number of cells with a luminescent output. Cells were seeded in a 12-well plate at ~10–30% confluency and inoculated with an MOI of 6. After 4 d of culture, cell viability was determined using the ratio of luminescence from the *Chlamydia*-infected clone to the luminescence from the uninfected clone.

Sulfate Labeling. Cells were seeded into six-well plates until they achieved ~70% confluency and 0.5 mCi/mL [^{35}S]SO$_4$ or 0.33 mCi/mL [^{35}S]methionine/[^{35}S] cysteine (PerkinElmer Life Sciences) was added to the media in each plate, and the cells were left to reach steady state for >24 h. A portion of each sample was harvested, lysed in Nonidet P-40, and then digested with heparitinase

(Seikagaku), chondroitinase ABC (Seikagaku), and PNGase F (New England BioLabs). Protein concentration was adjusted, the lysates were resolved on an SDS/PAGE gel, and the polypeptides were visualized by autoradiography.

1. Mandell GL, Bennett JE, Dolin R (2010) *Mandell, Douglas, and Bennett's Principles and Practice of Infectious Diseases* (Churchill Livingstone/Elsevier, Philadelphia), 7th Ed.
2. Hu VH, et al. (2010) Epidemiology and control of trachoma: Systematic review. *Trop Med Int Health* 15:673–691.
3. Dautry-Varsat A, Subtil A, Hackstadt T (2005) Recent insights into the mechanisms of *Chlamydia* entry. *Cell Microbiol* 7:1714–1722.
4. Zhang JP, Stephens RS (1992) Mechanism of *C. trachomatis* attachment to eukaryotic host cells. *Cell* 69:861–869.
5. Su H, et al. (1996) A recombinant *Chlamydia trachomatis* major outer membrane protein binds to heparan sulfate receptors on epithelial cells. *Proc Natl Acad Sci USA* 93:11143–11148.
6. Davis CH, Wyrick PB (1997) Differences in the association of *Chlamydia trachomatis* serovar E and serovar L2 with epithelial cells in vitro may reflect biological differences in vivo. *Infect Immun* 65:2914–2924.
7. Stephens RS, Poteralski JM, Olinger L (2006) Interaction of *Chlamydia trachomatis* with mammalian cells is independent of host cell surface heparan sulfate glycosaminoglycans. *Infect Immun* 74:1795–1799.
8. Carabeo RA, Hackstadt T (2001) Isolation and characterization of a mutant Chinese hamster ovary cell line that is resistant to *Chlamydia trachomatis* infection at a novel step in the attachment process. *Infect Immun* 69:5899–5904.
9. Fudyk T, Olinger L, Stephens RS (2002) Selection of mutant cell lines resistant to infection by *Chlamydia* spp [corrected]. *Infect Immun* 70:6444–6447.
10. Conant CG, Stephens RS (2007) *Chlamydia* attachment to mammalian cells requires protein disulfide isomerase. *Cell Microbiol* 9:222–232.
11. Elwell CA, Ceesay A, Kim JH, Kalman D, Engel JN (2008) RNA interference screen identifies Abl kinase and PDGFR signaling in *Chlamydia trachomatis* entry. *PLoS Pathog* 4:e1000021.
12. Gurumurthy RK, et al. (2010) A loss-of-function screen reveals Ras- and Raf-independent MEK-ERK signaling during *Chlamydia trachomatis* infection. *Sci Signal* 3:ra21.
13. Carette JE, et al. (2009) Haploid genetic screens in human cells identify host factors used by pathogens. *Science* 326:1231–1235.
14. Reiling JH, et al. (2011) A haploid genetic screen identifies the major facilitator domain containing 2A (MFSD2A) transporter as a key mediator in the response to tunicamycin. *Proc Natl Acad Sci USA* 108:11756–11765.
15. Carette JE, et al. (2011) Global gene disruption in human cells to assign genes to phenotypes by deep sequencing. *Nat Biotechnol* 29:542–546.
16. Papatheodorou P, et al. (2011) Lipolysis-stimulated lipoprotein receptor (LSR) is the host receptor for the binary toxin *Clostridium difficile* transferase (CDT). *Proc Natl Acad Sci USA* 108:16422–16427.
17. Qu X, et al. (2011) Lacrimal gland development and Fgf10-Fgfr2b signaling are controlled by 2-O- and 6-O-sulfated heparan sulfate. *J Biol Chem* 286:14435–14444.
18. Bhattacharya R, Townley RA, Berry KL, Bülow HE (2009) The PAPS transporter PST-1 is required for heparan sulfation and is essential for viability and neural development in *C. elegans*. *J Cell Sci* 122:4492–4504.
19. Jastrebova N, Vanwildemeersch M, Lindahl U, Spillmann D (2010) Heparan sulfate domain organization and sulfation modulate FGF-induced cell signaling. *J Biol Chem* 285:26842–26851.
20. Otsuki S, et al. (2010) Extracellular sulfatases support cartilage homeostasis by regulating BMP and FGF signaling pathways. *Proc Natl Acad Sci USA* 107:10202–10207.
21. Kehoe JW, Bertozzi CR (2000) Tyrosine sulfation: A modulator of extracellular protein–protein interactions. *Chem Biol* 7:R57–R61.
22. Hirata T, et al. (2004) Human P-selectin glycoprotein ligand-1 (PSGL-1) interacts with the skin-associated chemokine CCL27 via sulfated tyrosines at the PSGL-1 amino terminus. *J Biol Chem* 279:51775–51782.
23. Gutiérrez J, et al. (2004) Analysis of post-translational CCR8 modifications and their influence on receptor activity. *J Biol Chem* 279:14726–14733.
24. Choe H, et al. (2003) Tyrosine sulfation of human antibodies contributes to recognition of the CCR5 binding region of HIV-1 gp120. *Cell* 114:161–170.
25. Sasaki N, et al. (2009) The 3′-phosphoadenosine 5′-phosphosulfate transporters, PAPST1 and 2, contribute to the maintenance and differentiation of mouse embryonic stem cells. *PLoS ONE* 4:e8262.
26. Carette JE, et al. (2011) Ebola virus entry requires the cholesterol transporter Niemann-Pick C1. *Nature* 477:340–343.
27. Zaretzky FR, Pearce-Pratt R, Phillips DM (1995) Sulfated polyanions block *Chlamydia trachomatis* infection of cervix-derived human epithelia. *Infect Immun* 63:3520–3526.
28. Besset S, Vincourt JB, Amalric F, Girard JP (2000) Nuclear localization of PAPS synthetase 1: A sulfate activation pathway in the nucleus of eukaryotic cells. *FASEB J* 14:345–354.
29. Kamiyama S, et al. (2003) Molecular cloning and identification of 3′-phosphoadenosine 5′-phosphosulfate transporter. *J Biol Chem* 278:25958–25963.
30. Kamiyama S, et al. (2011) Expression and the role of 3′-phosphoadenosine 5′-phosphosulfate transporters in human colorectal carcinoma. *Glycobiology* 21:235–246.
31. Fadel S, Eley A (2004) Chlorate: A reversible inhibitor of proteoglycan sulphation in *Chlamydia trachomatis*-infected cells. *J Med Microbiol* 53:93–95.
32. Yabushita H, et al. (2002) Effects of chemically modified heparin on *Chlamydia trachomatis* infection of eukaryotic cells in culture. *Glycobiology* 12:345–351.
33. Bai X, Wei G, Sinha A, Esko JD (1999) Chinese hamster ovary cell mutants defective in glycosaminoglycan assembly and glucuronosyltransferase I. *J Biol Chem* 274:13017–13024.
34. Esko JD, Stewart TE, Taylor WH (1985) Animal cell mutants defective in glycosaminoglycan biosynthesis. *Proc Natl Acad Sci USA* 82:3197–3201.
35. Esko JD, et al. (1987) Inhibition of chondroitin and heparan sulfate biosynthesis in Chinese hamster ovary cell mutants defective in galactosyltransferase I. *J Biol Chem* 262:12189–12195.
36. Taraktchoglou M, Pacey AA, Turnbull JE, Eley A (2001) Infectivity of *Chlamydia trachomatis* serovar LGV but not E is dependent on host cell heparan sulfate. *Infect Immun* 69:968–976.
37. Kim JH, Jiang S, Elwell CA, Engel JN (2011) *Chlamydia trachomatis* co-opts the FGF2 signaling pathway to enhance infection. *PLoS Pathog* 7:e1002285.
38. Fadel S, Eley A (2008) Differential glycosaminoglycan binding of *Chlamydia trachomatis* OmcB protein from serovars E and LGV. *J Med Microbiol* 57:1058–1061.
39. Fadel S, Eley A (2007) *Chlamydia trachomatis* OmcB protein is a surface-exposed glycosaminoglycan-dependent adhesin. *J Med Microbiol* 56:15–22.
40. Stephens RS, Koshiyama K, Lewis E, Kubo A (2001) Heparin-binding outer membrane protein of chlamydiae. *Mol Microbiol* 40:691–699.
41. Chen Y, Götte M, Liu J, Park PW (2008) Microbial subversion of heparan sulfate proteoglycans. *Mol Cells* 26:415–426.
42. Bishop JR, Crawford BE, Esko JD (2005) Cell surface heparan sulfate promotes replication of *Toxoplasma gondii*. *Infect Immun* 73:5395–5401.
43. Rahuel-Clermont S, et al. (2010) Biochemical and thermodynamic characterization of mutated β1,4-galactosyltransferase 7 involved in the progeroid form of the Ehlers–Danlos syndrome. *Biochem J* 432:303–311.
44. Liu J, et al. (2008) Tyrosine sulfation is prevalent in human chemokine receptors important in lung disease. *Am J Respir Cell Mol Biol* 38:738–743.
45. Bernstein-Hanley I, et al. (2006) Genetic analysis of susceptibility to *Chlamydia trachomatis* in mouse. *Genes Immun* 7:122–129.